Microelectronics Reliability xxx (2014) xxx–xxx

Contents lists available at ScienceDirect

Microelectronics Reliability

journal homepage: www.elsevier.com/locate/microrel

Degradation transformation in spinel-type functional thick-film ceramic materials

H. Klym [a,*], V. Balitska [b,c], O. Shpotyuk [b,d], I. Hadzaman [e]

[a] Lviv Polytechnic National University, 12 Bandera str., Lviv 79013, Ukraine
[b] Lviv Institute of Materials of SRC "Carat", 202 Stryjska str., Lviv 79031, Ukraine
[c] Lviv State University of Life Safety, 35 Kleparivska str., Lviv 79007, Ukraine
[d] Jan Dlugosz University, 13/15 Al. Armii Krajowej, Czestochowa 42201, Poland
[e] Drohobych State Pedagogical University, 24 Ivan Franko str., Drohobych 82100, Ukraine

ARTICLE INFO

Article history:
Received 20 November 2013
Received in revised form 18 July 2014
Accepted 18 July 2014
Available online xxxx

Keywords:
Ageing
Degradation
Relaxation function
Thick films
Ceramics

ABSTRACT

The mathematical models of thermally-induced degradation processes in solids with nano- and micro-scale topological disordering – bulk and thick-film ceramic composites based on mixed transition-metal manganites are considered. It was shown that degradation transformations in these materials are best described by stretched or suppressed exponential relaxation function. The stretched exponential degradation kinetics is proper to own degradation transformations in such one-type systems as bulk ceramics and multilayered thick-film structures. The mechanism of degradation transformations in one-layered thick films, including two or more different on their origin elementary are described by suppressed exponential kinetics.

1. Introduction

It is well known that NTC thermistor based on Cu–Ni–Co–Mn oxyspinel systems exhibit a uniform exponential decrease of resistance with increasing temperature up to ~300 °C, which makes this compound well suited for use as a thermistor material in specific temperature sensors and attenuators [1]. Recent applications of these materials in LTCC microelectronics make thick-film production interesting [2–4]. The LTCC technology offers the interesting possibility to exploit the 3rd dimension in circuit printing "by sandwiching" several layers to produce a miniaturized multi-functional component [5]. It permits the integration of any kind of component, e.g. conductors, resistors, capacitors, inductors or attenuators into the integrated circuit element. However, the co-firing of multilayer systems is cost, time and size effective.

For commercial application where low-cost mass production is required, the screen-printing is the most suitable technological route for multilayer production. This technique has been well developed and industrially exploited extensively for making printed circuit boards, and more recently its use for the production of various thick-film sensors has been reported [6–9].

Our preliminary studies aimed on the development of technological route for thick-film thermistors fabrication were carried out indicating satisfactory NTC characteristics for fired films composed of $Cu_{0.1}Ni_{0.1}Co_{1.6}Mn_{1.2}O_4$ basic ceramics, Bi_2O_3 and glass [10]. Nevertheless, despite the well-pronounced NTC thermistor properties in the tested mixed transition-metal manganites in thick-film performance, some thick-film elements, at least of Co-enriched $Cu_{0.1}Ni_{0.1}Mn_{1.2}Co_{1.6}O_4$ composition, were non-stable against degradation, revealing a sharp relative resistance drift up to 10–15% yet in the first hours of ageing tests at $T < 200$ °C. This obstacle is absolutely inadmissible in the modern electronics and, consequently, it should be excluded by purposeful choice of the corresponding technological or post-technological modification methods. One of the possible resolutions was indicated at once by studying degradation kinetics of the observed ageing phenomena in the prepared thick films. It was shown particularly that after a certain ageing duration at the relatively low temperatures near 125–170 °C, the sharp initially-growing relative resistance drift curve did not saturate (as it was character for bulk ceramics) but only dropped down, tending slowly to 0.

As a rule, to eliminate parasitic influence of degradation effects in NTC electroceramics and thick films, the methods of their chemical modification by metallic additives at the initial stages of technological preparation have been usually used [11,12]. These metallic additives, being located near inter-granular regions in the

* Corresponding author. Tel.: +38 032 258 26 44; fax: +38 032 258 26 80.
E-mail address: klymha@yahoo.com (H. Klym).

http://dx.doi.org/10.1016/j.microrel.2014.07.137
0026-2714/

vicinity of grain boundaries, diminish thermally activated ageing phenomena by stabilizing intrinsic cationic distribution within individual grains. As a result, the modification of ceramic materials typically show a higher stability in comparison with non-modified ones. So the present paper is concerned with subsequent studies of a new ecological thick-film elements and structures (without Bi_2O_3 additives) based on modified $Cu_{0.1}Ni_{0.8}Co_{0.2}Mn_{1.9}O_4$ and $Cu_{0.1}Ni_{0.8}Co_{0.2}Mn_{1.9}O_4$ ceramics.

The high demands to functional reliability put forward an actual problem on exact description for degradation kinetics of the main exploitation parameters of NTC ceramics and thick-film structures, such as electrical resistance R and thermal constant B. In spite of a great number of experimental research fulfilled under different kinds of ceramic materials with well pronounced TR effect, the precise functional expression corresponding to their ageing kinetics has not been established up to now. This disadvantage is accepted especially sharp in comparison with a number of analytical functions available for time-dependent ageing phenomena in other topologically disordered solids [13–16].

The aim of this work is mathematical description of degradation processes in modified thick-film structures and spinel-based NTC ceramic, taking into account main principles of the previously developed general approach to similar phenomena in other topologically disordered solids with using of relaxation functions [13].

2. Relaxation functions for description of degradation processes

In is known that degradation processes or time-dependent "drift" of control parameter η in topologically-disordered materials (for example glass, ceramics and thick films) with tendency to thermodynamically equilibrium state can be described by using general differential equation $\frac{d\eta}{dt} = -\lambda\eta^{\alpha}t^{\beta}$ (for monotonically decreasing degradation kinetics) and $\frac{d\eta}{dt} = \lambda(1-\eta)^{\alpha}t^{\beta}$ (for monotonically increasing degradation kinetics), where t is process duration, α and β are material-related constants. Differential equations for monotonically decreasing and increasing degradation kinetics and corresponding boundary conditions are shown in Table 1. Analytical degradation kinetics are described by so-called relaxation function (*RF*), i.e. normalized mathematical function $N_\eta(t)$ or $M_\eta(t) = 1 - N_\eta(t)$ containing the exact solution of the above differential equations $\eta(t)$.

As it is shown early [17,18], there are 5 typical solutions of the above differential equation in dependence on α and β numerical values. Each of them contains a basic t-dependent functional *RF*. The *RF* is numerically equal to relative change in the control parameter η in the moment t being presented typically in the normalized form (i.e. within 0–1 domain).

At the case of $\alpha = 1$ and $\beta = 0$, the simple exponential monomolecular *RF*-1 ($N_\eta(t) = \exp\left(-\frac{t}{\tau}\right)$, where $\tau = \frac{1}{\lambda}$, $\eta_0 = \exp(c)$, c = constant, $\lambda \neq 0$) is valid. This function is used for description of activation processes determined by one prevailing value of activation energy into more equilibration state (the similar processes can be observed, as a rule, in crystalline).

If ageing processes is caused by recombination of specific defect pairs (electrons and holes, interstitials and vacancies, etc.), their degradation is determined by bimolecular *RF*-2 at $\alpha = 2$ and $\beta = 0$ ($N_\eta(t) = \exp\left(1 + \frac{t}{\tau}\right)^{-1}$, where $\tau = \frac{1}{\lambda}$, $\eta_0 = \exp(c)$, c = constant, $\lambda \neq 0$). The strict resolution of degradation equation at $\alpha \neq 0$ and $\beta = 0$ can be presented in the form of partly-generalized *RF*-3. ($N_\eta(t) = \exp\left(1 + \frac{t}{\tau}\right)^{-k}$, where $\tau = \frac{c}{\lambda(\alpha-1)}$, $\eta_0 = c^{1/(\alpha-1)}$ $k = \frac{1}{\alpha-1}$, c = constant, $\alpha \neq 0$, $\lambda \neq 0$). This function is often used for description of thermally-induced effects in some oxide glasses. In the case at $\alpha = 1$ and $\beta \neq 0$, the ageing kinetics is defined by stretched-exponential *RF*-4 ($N_\eta(t) = \exp\left[\left(-\frac{t}{\tau}\right)\right]^{k}$, where $\tau = \frac{1+\beta}{\lambda}$, $k = 1 + \beta$, $\eta_0 = \exp(c)$, c = constant, $\beta \neq -1$ $\lambda \neq 0$), the most adequate mathematical function for structural, mechanical and electrical relaxation in a large number of topologically-disordered solids (mostly in glass and ceramic-based materials). The exact solution of the general degradation equation is given by fully-generalized *RF*-5 at $\alpha \neq 0$ and $\beta \neq 0$ ($N_\eta(t) = \exp\left[\left(1 + \frac{t}{\tau}\right)^{-k}\right]^{r}$, where $\tau = \left[\frac{1+\beta}{\lambda(\alpha-1)}\right]^{\frac{1}{1+\beta}}$, $k = 1 + \beta$, $r = \frac{1}{\alpha-1}$, $\eta_0 = c^{1/(1-\alpha)}$, c = constant, $\alpha \neq 1$ $\beta \neq -1$ $\lambda \neq 0$).

Table 1
Differential equations and corresponding boundary conditions describing of decreasing and increasing degradation kinetics.

Decreasing degradation kinetics	Increasing degradation kinetics
$\frac{d\eta}{dt} = -\lambda\eta^{\alpha}t^{\beta}$	$\frac{d\eta}{dt} = \lambda(1-\eta)^{\alpha}t^{\beta}$
$\begin{cases} t \to 0 \Rightarrow \eta \to \eta_0 \\ t \to \infty \Rightarrow \eta \to 0 \end{cases}$; $N_\eta(t) = \frac{\eta_t - \eta_\infty}{\eta_0 - \eta_\infty}$	$\begin{cases} t \to 0 \Rightarrow \eta \to 0 \\ t \to \infty \Rightarrow \eta \to \eta_0 \end{cases}$; $M_\eta(t) = 1 - N_\eta(t)$

But at $\alpha = 1$ and arbitrary β value, all *RF*s are exponential ones, since their t-dependences attain a character exponential form with index (or functional) $N_\eta(t) \sim \exp\left[-\left(\frac{t}{\tau}\right)\right]^{k}$. Within this approach, the τ value in the above functional is numerically equal to the time domain, which corresponds to e-times decrease in the control parameter η, provided k tends to 1: $\tau = \frac{1+\beta}{\lambda} = \frac{k}{\lambda}$. If β parameter equals 0 (or, equivalently, if $k = 1$), the *RF*-2 transforms into ideal exponential *RF* called sometimes the monomolecular or Debye RF [13]: $N_\eta(t) \sim \exp\left[-\left(\frac{t}{\tau}\right)\right]$.

The relaxation constant τ is introduced only for the above ideal exponential ageing or degradation process. Despite numerical coincidence, the τ parameter in the functional is not relaxation constant in a strong meaning of this term [19].

Monomolecular degradation kinetics is a characteristic of activating processes in solids describing thermodynamics equilibration state through one certain parameter. These processes are determined by one unique or one prevailing value of activating energy, not disturbed by dispersive additional factors (first of all structural). It is quite understandable, that these processes are observed in crystallographically ordered solids (single- and polycrystalline).

The exponential *RF*-4 is not applied for relaxation processes in dispersive substances. Nevertheless, it unexpectedly gave a quite good result for simulation of degradation kinetics of electro-induced dichroism in vitreous arsenic trisulfide [19]. This result testifies that in spite of dispersive character in atomic structure of chalcogenide glasses caused by short- and medium-range ordering structural fluctuations (lengths and angles of covalent chemical bonds, distances between directly non-bonding atoms and more extended atomic blocks, etc.) [17], defect centres responsible for this effect annihilate with one primary value of activation energy. This energy seems to be close to the dissociation energy of covalent chemical bonds forming the glassy-like network.

In some cases the degradation kinetics appears as a consequence of simultaneous contribution of several individual relaxation processes. In this case, the total degradation process, naturally, is an exponential-like one being adequately described by linear combination of individual functional with a set of independent relaxation times τ. The overall number of constituent *RF*s can be a large enough in dependence on the type of the investigated system. So, in particular, Kovacs A.J., Hutchinson J.M. and Aklonis J.J. shown that the relaxation kinetics described by *RF*-2 with power-like index $k = 0.455$ can be transferred into more optimal function, containing as high as 33 simple exponential components like to *RF*-4 [20].

Please cite this article in press as: Klym H et al. Degradation transformation in spinel-type functional thick-film ceramic materials. Microelectron Reliab (2014), http://dx.doi.org/10.1016/j.microrel.2014.07.137

Table 2
Standard deviations (*err*) for different *RF*s, describing ageing processes in $Cu_{0.1}Ni_{0.1}Co_{1.6}Mn_{1.2}O_4$ bulk ceramics, *p*-conductive $Cu_{0.1}Ni_{0.8}Co_{0.2}Mn_{1.9}O_4$ thick films and p^+–*p* thick-film structure.

Sample	*err*				
	RF-1	*RF*-2	*RF*-3	*RF*-4	*RF*-5
Bulk ceramics [25]	0.402	0.129	0.047	0.017	0.023
p^+–*p* Thick-film structure	0.274	0.090	0.023	0.021	0.021
p-Conductive thick films	0.437	0.990	0.025	0.037	0.038

3. Stretched and suppressed exponential degradation kinetics

If $0 < k < 1$, the *RF*-4 attains a so-called extended or stretched exponential character describing the chosen ageing process assuming a continuous spectrum of relaxation times. Many authors call this *RF* "stretched-exponential" [21]. However, this term seems be not quite ideal. Other alternative terms can be met in the specialized literature, using, in part, the names of authors firstly applied this *RF*. Thus, this function is used as Williams-Watts function after the names of authors, which applied it to describe the dielectric relaxation kinetics in polymethylmethacrylate [16]. Another alternative term is the De Bast–Gilard RF after the names of authors, used this function to describe the mechanical stress relaxation in glasses [15]. As for us, the best term for this *RF* is the Kohlrausch function, who was the first applied it for relaxation processes in complex electronic and molecular systems [22]. The combined term of this *RF* are also met (in the form of KWW or Kohlrausch–Williams–Watts function) [23].

The mechanisms of degradation processes in topologically-disordered systems describing of stretched exponential relaxation kinetics are quite different. Two main groups can be distinguished among them. The first group explores mechanisms in terms of dispersive transport in disordered structures [24]. The character defects in these structures responsible for a deviation from thermodynamic equilibration state in multiple capture-elimination acts of excited carriers before finally stabilized within degradation test. The quantitative parameters of elementary capture and elimination acts form a continuous spectrum in agreement with structural disordering of solid system. The model of hierarchically limited relaxation dynamics is in the ground of the second group of mechanisms. Within this model, each individual relaxation transformation in disordered solids is possible after previous relaxation events, formed the favourable conditions for its realization (as free-volume space).

It should be noted that all parameters in the stretched exponential *RF* carry their strongly-defined physical meanings. Thus, the k index in functional $N_\eta(t) \sim \exp\left[-\left(\frac{t}{\tau}\right)\right]^k$ determines the time width of relaxation process. It is shown [25,26] that stretched exponential behavior corresponds to more smooth decaying of control parameter $\eta(t)$ in the region of short times $\left(\frac{t}{\tau} < 1\right)$ and more late decaying in the region of long times $\left(\frac{t}{\tau} > 1\right)$ in comparison with simple exponential *RF* obtained at $k = 1$. With other words, the ideal exponential curve $\eta(t) \sim \exp\left[-\left(\frac{t}{\tau}\right)\right]$ by transforming into stretched-exponential ones extends in time, tending asymptotically to straight line with $k = 0$.

Taking into account that stretched exponential *RF* corresponds to relaxation kinetics in supposition on dispersive transport in disordered systems [24]. It should be expected that it will be the most optimal one to describe the degradation kinetics in electrophysical properties of variable-composition materials, provided these phases are identical in their origin. It means that kinetic curves of ageing processes for one-type topology-disordered systems (for example, ceramic composites sintered at high temperatures, covalent-bonded network glasses quenched from a melt, thick-film structures with different conductivity of layers, etc.) will be attain a character extended behavior proper to the stretched exponential *RF* with $0 < k < 1$.

The second resolution of general differential equation of degradation $\frac{d\eta}{dt} = -\lambda\eta^a t^\beta$ can be obtained a so-called suppressed exponential *RF* as a subject to the condition $\kappa > 1$. This kind of kinetics corresponds to smaller changes in control parameter $\eta(t)$ at $\left(\frac{t}{\tau} < 1\right)$ and considerably greater changes at $\left(\frac{t}{\tau} > 1\right)$. The observed degradation kinetics attains a specific threshold-like shape, i.e. the changes of the controlled parameter $\eta(t)$ are negligible in the beginning and in the end of degradation test.

Probably, such behavior is proper to complex physical processes in topology-disordered solids, which include two and more elementary components of principally different origin. Diffusion, evaporation, adsorption, burning-out of inner phase inclusions, chemical interaction between main phase and impurities, etc. can serve as typical examples of the above processes in ceramics. These processes are needed a different energies for their realization. In addition, they are time-interdependent, since each next component occurs only after previous ones. In other words, the main relaxation process in the region of $\frac{t}{\tau} = 1$ begins only after a certain preparation stage with essentially less activation energy.

4. Results and discussion

For study of thermally-induced ageing we selected samples of $Cu_{0.1}Ni_{0.1}Co_{1.6}Mn_{1.2}O_4$ bulk ceramics, *p*-conductive $Cu_{0.1}Ni_{0.8}Co_{0.2}Mn_{1.9}O_4$ thick films and p^+–*p* thick-film structures based on *p*-conductive $Cu_{0.1}Ni_{0.8}Co_{0.2}Mn_{1.9}O_4$ and p^+-conductive $Cu_{0.1}Ni_{0.1}Mn_{1.2}Co_{1.6}O_4$ ceramics. The investigated $Cu_{0.1}Ni_{0.1}Co_{1.6}Mn_{1.2}O_4$ bulk ceramics were sintered at maximum temperature of 1200 °C and contained three phases – the base spinel-type phase of the above composition, the Co-enriched rock-salt phase and slight remainders of non-identified

Table 3
Fitting parameters for different *RF*s, describing ageing processes in $Cu_{0.1}Ni_{0.1}Co_{1.6}Mn_{1.2}O_4$ bulk ceramics, *p*-conductive $Cu_{0.1}Ni_{0.8}Co_{0.2}Mn_{1.9}O_4$ thick films and p^+–*p* thick-film structure.

Sample	*RF*-1		*RF*-2		*RF*-3		
	η_0	τ	η_0	τ	η_0	τ	κ
Bulk ceramics	6.58	34.9	7.25	24.9	16.91	1.90	0.10
p^+–*p* Thick-film structure	5.48	17.3	6.07	12.4	10.02	1.95	0.19
p-Conductive thick films	7.90	11.6	8.60	7.6	12.06	0.24	1.10
Sample	*RF*-4			*RF*-5			
	η_0	τ	κ	η_0	τ	κ	r
Bulk ceramics	10.9	359.5	0.29	7.91	139.1	1.29	0.62
p^+–*p* Thick-film structure	7.42	56.4	0.38	14.37	2.71	0.60	0.20
p-Conductive thick films	9.14	16.9	0.40	12.80	0.80	2.27	0.09

Please cite this article in press as: Klym H et al. Degradation transformation in spinel-type functional thick-film ceramic materials. Microelectron Reliab (2014), http://dx.doi.org/10.1016/j.microrel.2014.07.137

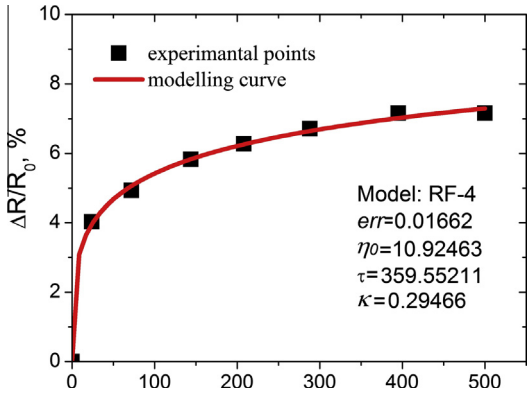

Fig. 1. Thermally-induced (170 °C) relative resistance drift ($\Delta R/R_0$) in bulk $Cu_{0.1}Ni_{0.1}Co_{1.6}Mn_{1.2}O_4$ ceramics described by *RF*-4.

phase (probably NiO) [10]. Temperature sensitive *p*-conductive $Cu_{0.1}Ni_{0.8}Co_{0.2}Mn_{1.9}O_4$ and p^+-conductive $Cu_{0.1}Ni_{0.1}Mn_{1.2}Co_{1.6}O_4$ pastes were prepared by mixing powders of basic ceramics (sintered bulk ceramic discs were preliminary crushed, wet-milled in isopropyl alcohol medium and dried) with ecological glass powder, Bi_2O_3 (inorganic binder) and an organic components (organic binder and organic solvent) [29–31]. The *p*-conductive thick films and their p^+–*p* structures based on *p*-conductive $Cu_{0.1}Ni_{0.8}Co_{0.2}Mn_{1.9}O_4$ and p^+-conductive $Cu_{0.1}Ni_{0.1}Mn_{1.2}Co_{1.6}O_4$ ceramics have been printed on alumina substrates (Rubalit 708S) with Ag electrodes and sintered at 850 °C during 15 min with future decreasing of temperature. The total duration of technological process was 45 min. This is not enough time for obtaining of single-phase thick-film composition. Finally, the studied thick-film samples were a complex solid-state system comprising of contact between the Ag electrodes and thick films with crystalline grains of the main phase, small amount of glass additives and non-evaporated remnants of carbon components, which nonexceed 0.01% in total amount of the solid materials [10]. Multilayered p^+–*p* thick-film structures were obtained by printing of paste in two layers on a substrate.

Long-term ageing test was carried out at 170 °C for study of thermo-stability of spinel-type functional $Cu_{0.1}Ni_{0.8}Co_{0.2}Mn_{1.9}O_4$ ceramics [27], *p*-conductive $Cu_{0.1}Ni_{0.8}Co_{0.2}Mn_{1.9}O_4$ thick films and p^+–*p* thick-film structures [28–31]. The total duration of the degradation transformation was 500 h for bulk ceramics and 250 h for thick films and thick-film structures [32]. Measurements of electrical resistance *R* were carried out at 25 °C after successive thermotreatment stages. The values of relative change (drift) of electrical resistance $\eta = \Delta R/R_o$ (where R_o is initial value of electrical resistance and ΔR – absolute change of electrical resistance caused by the degradation test) were selected as controlled parameters [33].

For adequate mathematical description of the experimentally observed degradation kinetics, as well as the establishment of possible microstructural mechanisms, we have developed a software package for modeling of thermally-induced ageing processes in ceramic materials using fitting parameters of *RF*s. The values of fitting parameters are selected for minimization of mean-square deviations (*err*) of experimental values of drift on theoretical curve corresponding to *RF*s. Conclusion on the possible mechanism of degradation processes is carried out based on sequence analysis of *RF*s containing minimum number of fitting parameters.

The experimental curves and modeling results of degradation processes for studied functional materials by using of five *RF*s are shown in Tables 2 and 3, Figs. 1–3. Monomolecular *RF*-1 is evaluated by simplest exponential dependence, but the *err* value (as in *RF*-2 and at times in *RF*-3) is significantly higher than corresponding value for *RF*-4 and *RF*-5 at fitting parameters η_0, τ, κ and *r* (for

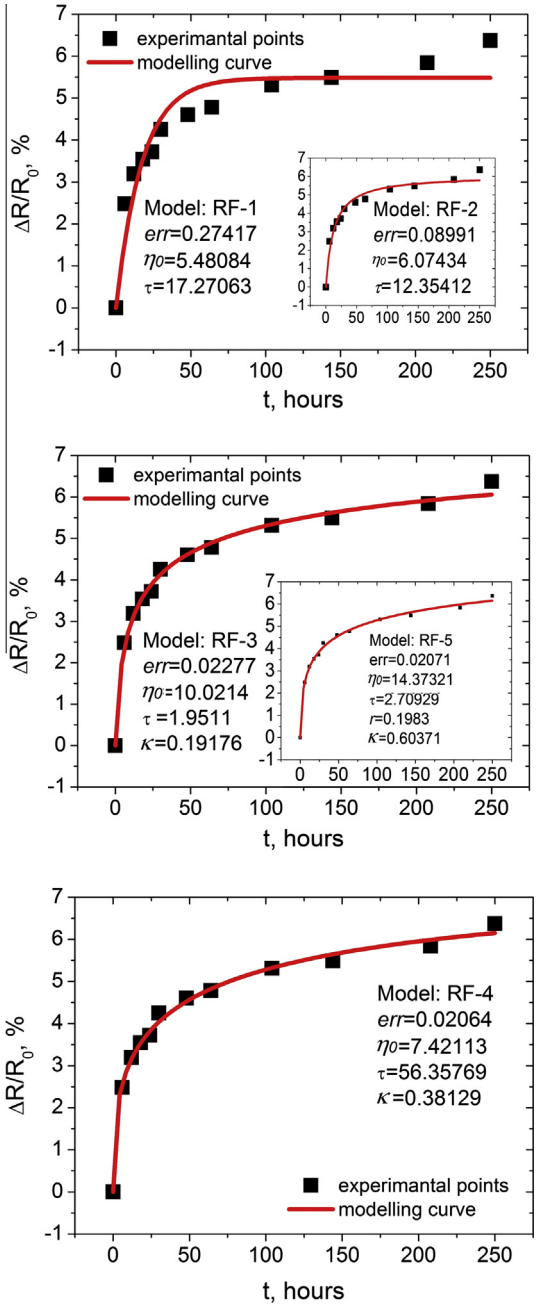

Fig. 2. Thermally-induced (170 °C) relative resistance drift ($\Delta R/R_0$) in p^+–*p*-conductive thick film structures described by increasing degradation kinetics.

RF-5). As to kinetics of these relaxation transformations, the parameter η_0 rate of the relaxation processes, κ – dependent strongly on grain-pore morphology of the ceramics and thick films (also defined by amount of edition phases presenting into ceramic materials) and the effective time constant τ occurs to be inversely related to relative drift of electrical resistance. So the quicker relaxation process causes more pronounced degradation in electrical resistance. The parameter *r* is additional fitting parameter without physical meaning.

The fitting of experimentally observed degradation kinetics by *RF*-4 is shown to be most optimal in terms of mean-square deviations (the smallest *err* values in comparison with other *RF*s). It should be noted that fitting route with *RF*-5 gives also a quite good correspondence, but this function is not optimal one in view of large number of fitting parameters. The *err* value for *RF*-3 is not

Please cite this article in press as: Klym H et al. Degradation transformation in spinel-type functional thick-film ceramic materials. Microelectron Reliab (2014), http://dx.doi.org/10.1016/j.microrel.2014.07.137

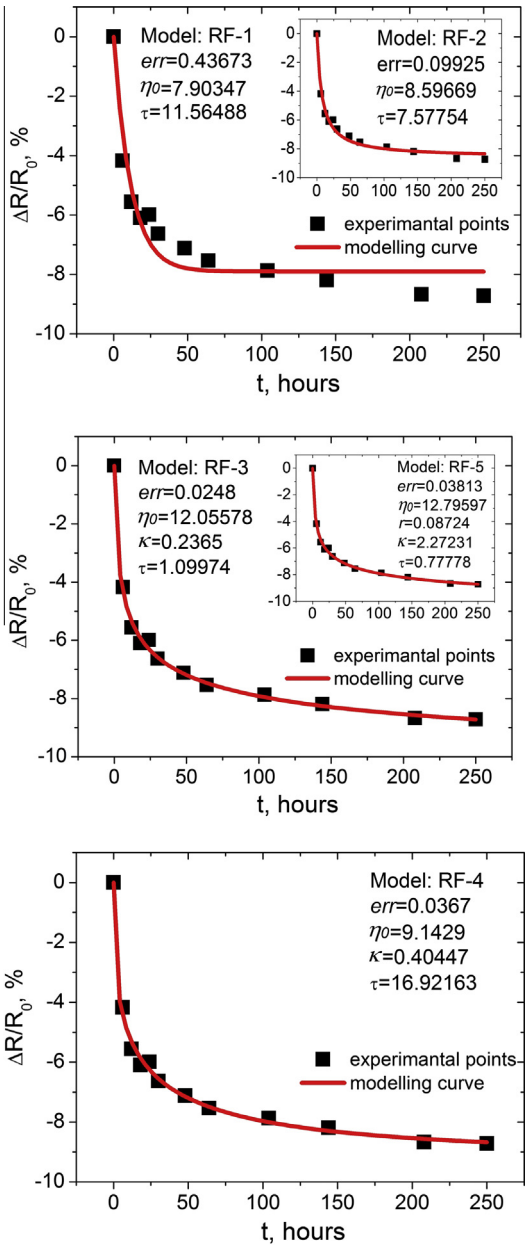

Fig. 3. Thermally-induced (170 °C) relative resistance drift ($\Delta R/R_0$) in *p*-conductive $Cu_{0.1}Ni_{0.8}Co_{0.2}Mn_{1.9}O_4$ thick films described by decreasing degradation kinetics.

so much, but this relaxation function is used mainly for description of thermally-induced processes in oxide glasses.

Taking into account, that the *RF*-4 corresponds to kinetics of relaxation processes in disordered media [34], it is clear that it was most appropriate to describe the kinetic dependence of degradation electrical properties of disordered materials with topologically different phase composition, provided uniformity the origin of these phases. Therefore, our future analysis we focus mainly on the *RF*-4 in stretched and suppressed exponential forms.

The degradation kinetics of relative resistance drift ($\Delta R/R_0$) in spinel-type $Cu_{0.1}Ni_{0.1}Co_{1.6}Mn_{1.2}O_4$ bulk ceramics and p^+–p thick-film structures caused by long-term ageing test at 170 °C are shown in Figs. 1 and 2. The investigated ceramics contained three phases – the base spinel-type phase of the above composition, the Co-enriched rock-salt phase and slight remainders of non-identified phase (probably NiO) [10]. Despite three phases in the final chemical composition, they are fully identical in their origin because of high sintering temperature of ceramics (1200 °C). So, the investigated samples can be considered as typical representative of uniform one-type topology-disordered system. The p^+-conductive $Cu_{0.1}Ni_{0.1}Co_{1.6}Mn_{1.2}O_4$ and *p*-conductive $Cu_{0.1}Ni_{0.8}Co_{0.2}Mn_{1.9}O_4$ thick films contain crystalline spinel phase with some glass additives and extremely small amount organic (carbon-based) components (near 0.001%) non-evaporated during degradation test [27].

As it exemplified from Fig. 1, the observed thermally-induced ageing curve for ceramics has a character sharp-growing shape in the first 100–200 h of ageing test with following slow tending to relative saturation at more prolonged storage (400–500 h). The maximal value of relative resistance drift is as high as 6–7%. The degradation curve for p^+–p thick-film structures in the first 50–150 h increases with future stabilization during degradation test (Fig. 2). The maximum value of electrical resistance drift is near 6%, like for bulk ceramics.

The ageing kinetics in the investigated $Cu_{0.1}Ni_{0.1}Co_{1.6}Mn_{1.2}O_4$ bulk ceramics and p^+–p thick-film structures can be well described by stretched-exponential kinetics *RF*-4. Indeed, in this case, the low values of *err* (Table 2) are achieved at a relatively small number of fitting parameters (η_0, τ, κ). Parameters η_0 and τ decrease in thick-film structures in comparison with bulk ceramics (Table 3). The mechanism of thermally-induced transformation is assumed to be identical in monolithic ceramics and thick-film structures are caused by availability of additional phases and grain-pore morphology (reflected by parameter κ). The difference consists in quantitative parameters of the change in electrical resistance (parameter τ). Low porosity of p^+–p structures [29] exhibits increasing of parameter κ without regard to small amount of additional phases in comparison with three-phase bulk ceramics. The similar results were obtained for some other ceramic samples within mixed transition-metal manganite system $Cu_xNi_{1-x-y}Co_{2y}Mn_{2-y}O_4$ [32]. It should be note that this result is valid, while the microstructural mechanism associated with ageing carries a complicated character, including not only cation redistribution, but also interphase mass-exchanging processes [27].

In addition, proposed in this work stretched-exponential relaxation kinetics model can be used for describing of long-term degradation transformation in other temperature-sensitive materials (such as NTC planar thermistor (based on $Mn_{1.6}Co_{0.8}Ni_{0.35}Ru_{0.25}O_4$ system made on alumina or LTCC substrates using thick-film procedure) fabricated and studied by Dziedzic and Prociow in [5]). Long term stability was characterized by measurements the relative resistance changes of thermistors up to 500 h at 150 °C. The results were also controlled by relative resistance drift values $\Delta R/R_0$. The value of this parameter drift is from 1.2% to 22% in dependence of substrate, position of thermistor and its area.

The ageing kinetics in such NTC thermistors can be described by increasing degradation kinetics using examined *FR*s. The approximate analyses of experimental results of degradation kinetics presented in [5] by five *RF*s is shown, that the most optimal in terms of mean-square deviations is *FR*-4. This suggests that mechanism of thermally-induced transformation in such NTC thermistors is a similar to monolithic spinel ceramics and multilayered thick-film structures caused by their composition and grain-pore morphology.

So, the stretched-exponential relaxation kinetics dominates in thermistor materials in bulk and thick-film performance in spite of their chemical composition, provided all phases formed during their sintering have one-type origin.

The character of degradation transformation in *p*-conductive thick films is other (Fig. 3). Proper thermo-induced structure changes of these samples are extremely small and offset against the more important processes. In result, instead of a positive change of $\Delta R/R_0$ (like in bulk ceramics and multilayered thick-film structures), the "negative" effect of decreasing of electrical

Please cite this article in press as: Klym H et al. Degradation transformation in spinel-type functional thick-film ceramic materials. Microelectron Reliab (2014), http://dx.doi.org/10.1016/j.microrel.2014.07.137

resistance is shown for studied $Cu_{0.1}Ni_{0.8}Co_{0.2}Mn_{1.9}O_4$ thick films. Using the procedure of finding the optimal analytical solutions of differential equations of general degradation, it was found that the kinetics of this effect is uniquely described by the suppressed exponential *RF*-4 [25].

Electron microscopy study of thick films before and after degradation transformation shown penetration depth of metallic Ag into thick films localized mainly near grain boundaries as well as additional glass phase [10,29,31]. Consequently, two interconnected foreign processes are activated in these materials during ageing: burning of organic binder from grain boundaries and penetration of metallic Ag into vacant space. As a result, the resistance of the thick films is decreased not only by improving the grain contacts (i.e. compacting of the films), but also due to appearance of intergranular space in the conductor. Such behavior of kinetics correspond to smaller changes in controlled parameter. The time interval of the relaxation process is reduced. Parameter κ is higher in comparison with bulk ceramics and p^+–p thick-film structures due to addition diffusion processes in one-layered thick films.

5. Conclusion

Thermally-induced degradation processes in functional bulk ceramics, thick films and multilayered thick-film structures can be described by using of exponential relaxation functions. It is shown that these processes are most adequately described by *RF*-4. Stretched exponential kinetic characterizes own degradation transformation in systems similar in nature (peculiar to bulk ceramics and multilayered thick-film structures). Ageing performance including two or more elementary and fundamentally different in origin processes are described by suppressed exponential *RF*-4 (peculiar to one-layered thick films).

References

[1] Sheftel IT. Thermoresistors. Moscow: Nauka; 1973.
[2] Feingold AH, Wahlers RL, Amstutz P, Huang C, Stein SJ. New microwave applications for thick-film thermistors. Microwave J 2000;43:90–8.
[3] Zhong J, Bau HH. Thick film thermistors printed on low temperature co-fired ceramic tapes. Am Ceram Soc Bull 2001;80(10):39–42.
[4] Dziedzic A, Golonka L, Hrovat M, Kita J, Belavič D. LTCC resistors and resistive temperature sensors – chosen electrical and stability properties. Proc 28th Int Spring Seminar Electr Technol 2005:165–70.
[5] Dziedzic A, Prociow EL. Some remarks about planar thermistors. Proc 25th Int Spring Seminar Electr Technol 2002:114–7.
[6] Qu W, Green R, Austin M. Development of multi-functional sensors in thick-film and thin-film technology. Meas Sci Technol 2000;11:1111.
[7] White NW, Turner J. Thick-film sensors: past, present and future. Meas Sci Technol 1997;8:1–4.
[8] Dziedzic A, Golonka LJ, Kozlowski J, Licznerski DW, Nitsch K. Thick-film resistive temperature sensors. Meas Sci Technol 1997;8:78.
[9] Prudenziati M, Morten B. Thick-film sensors: an overview. Sens. Actuators 1986;10:65–82.
[10] Brunets I, Mrooz O, Shpotyuk O, Altenburg H. Thick-film NTC thermistors based on spinel-type semiconducting electroceramics. Proc 24th Int Conf Microelectr 2004;2:503–6.
[11] Metz R, Brieu M, Legros R, Rousset A. Intergranular phases in electroceramics. Colloque de Phys 1990;51:1003–8.
[12] Castelan P, Loubiere A, Rousset A, Legros R. Ageing study of nickel–copper–manganite negative temperature coefficient thermistors by thermopower measurements. J Appl Phys 1992;72:119–22.
[13] Mazurin IV. Relaxation phenomena in glass. J Non-Cryst Solids 1977;25:130–69.
[14] Balitska VO, Shpotyuk OI, Vakiv MM. Degradation of electron-induced dichroism in glassy As_2S_3–Sb_2S_3. Ukr J Phys Opt 2000;1:107–10.
[15] De Bast J, Gilard P. Variation of the viscosity of glass and relaxation of stresses during stabilization. Phys Chem Glasses 1963;4:117–28.
[16] Williams G, Watts DC. On-symmetrical dielectric relaxation behavior arising from a simple empirical decay function. Trans Faraday Soc 1970;66:80–5.
[17] Balitska VO, Butkievich B, Shpotyuk OI, Vakiv MM. On the analytical description of ageing kinetics in ceramics manganite-based NTC thermistors. Microelectron Reliab 2002;42:2002–7.
[18] Hilfer R. Analytical representations for relaxation functions of glasses. J Non-Cryst Solids 2002;305:122–6.
[19] Felts A. Amorphous and vitreous inorganic solids. Moscow: Mir; 1986.
[20] Kovacs AJ, Hutchinson JM, Aklonis JJ. Isobaric volume and enthalpy recovery of glasses. I. A critical survey of recent phenomenological approaches. The structure of non-crystalline materials, London; 1977. p. 167–72.
[21] Corsaro RD. Volume relaxation of dry and wet boron trioxide in the glass transformation range following a sudden change of pressure. Phys Chem Glasses 1976;17:13–22.
[22] Kohlrausch F. Uber die elastische nachwirkung bei der torsion. Pogg Ann 1863;119:337–68.
[23] Gomez D, Alegria A. On the empirical functions describing the relaxation of glass-forming systems. J Non-Cryst Solids 2001;287:246–51.
[24] Emelianova EV, Hertogen P, Arkhipov VI, Adriaenssens GI. A model of photoinduced anisotropy in chalcogenide glasses. J Non-Cryst Solids 2000;266–269:954–8.
[25] Klym H, Balitska V, Vakiv M. On the non-exponential degradation kinetics in topologically-disordered substances. Prace Naukowe. Chemia i Ochrona Środowiska. Akademia im. Jana Długosza w Częstochowie 2005;10:33–43.
[26] Phillips JC. Stretched exponential relaxation in monomolecular and electronic glasses. Rep Prog Phys 1996;59:1133–207.
[27] Shpotyuk O, Balitska V, Hadzaman I, Klym H. Sintering-modified mixed Ni–Co–Cu oxymanganospinels for NTC electroceramics. J Alloys Compd 2011;509:447–50.
[28] Klym H, Hadzaman I, Shpotyuk O, Brunner M. Integrated thick-film nanostructures based on spinel ceramics. Nanoscale Res Lett 2014;9:149-1–6.
[29] Klym H, Hadzaman I, Shpotyuk O, Fu Q, Luo W, Deng J. Integrated thick-film p–i–p^+ structures based on spinel ceramics. Solid State Phenom 2013;200:156–61.
[30] Hadzaman I, Klym H, Shpotyuk O. Nanostructured oxyspinel multilayers for novel high-efficient conversion and control. Int J Nanotechnol 2014;11:843–53.
[31] Klym H, Hadzaman I, Ingram A, Shpotyuk O. Multilayer thick-film structures based on spinel ceramics. Can J Phys 2014;92:1–5 [in press].
[32] Vakiv M, Shpotyuk O, Mrooz O, Hadzaman I. Controlled thermistor effect in the system $Cu_xNi_{1-x-y}Co_{2y}Mn_{2-y}O_4$. J Eur Ceram Soc 2001;21:1783–5.
[33] Vakiv MM, Shpotyuk OI, Balitska VO, Butkievich B, Shpotyuk LI. Ageing behavior of electrical resistance in manganite NTC ceramics. J Eur Ceram Soc 2004;24:1243–6.
[34] Klym H. Peculiarities of non-exponential degradation kinetics in topology-disordered solids. In: Proceedings of the international conference TCSET'2006. Modern problems of radio engineering, telecommunications and computer science; 2006. p. 68–71.

Please cite this article in press as: Klym H et al. Degradation transformation in spinel-type functional thick-film ceramic materials. Microelectron Reliab (2014), http://dx.doi.org/10.1016/j.microrel.2014.07.137